NANOSYSTEMS: PHYSICS, CHEMISTRY, MATHEMATICS, 2020, 11 (4), P. 462–467

Solubility phase equilibrium in ternary system fullerenol $C_{60}(OH)_{24}$ and praseodymium salt: $PrCl_3$–$C_{60}(OH)_{24}$–H_2O at 25 °C

G. A. Glushnev[1], Ayat Kanbar[1], V. A. Keskinov[1], N. A. Charykov[1,2], K. N. Semenov[1,4,6], Z. K. Shaimardanov[3], B. K. Shaimardanova[3], N. A. Kulenova[3], D. G. Letenko[5]

[1]St. Petersburg State Technological Institute (Technical University), Moskovsky prospect, 26, St. Petersburg, 190013, Russia
[2]St. Petersburg Electrotechnical University "LETI", ul. Professora Popova 5, 197376 St. Petersburg, Russia
[3]D. Serikbayev East Kazakhstan state technical university, A. K. Protozanov Street, 69, Ust-Kamenogorsk, 070004, The Republic of Kazakhstan
[4]St. Petersburg State University, 7/9 Universitetskaya emb., St. Petersburg, 199034, Russia
[5]St.Petersburg State University of Architecture and Civil Engineering (SPSUACE), 2nd Krasnoarmeiskaya St. 4, 190005 St. Petersburg, Russia
[6]Pavlov First St. Petersburg StateMedical University L'va Tolstogo str. 6–8 St. Petersburg, 197022, Russia
keskinov@mail.ru

PACS 61.48.+c **DOI 10.17586/2220-8054-2020-11-4-462-467**

Solubility diagram was investigated by the method of saturation in ampules at 25 ± 0.02 °C for 4 hours. The solubility diagram of the $PrCl_3$–$C_{60}(OH)_{24}$–H_2O ternary system at 25 °C occurs as simple eutonics, consisting of two branches, corresponding to the crystallization of crystal-hydrates: $PrCl_3 \cdot 7H_2O$ and $C_{60}(OH)_{24} \cdot 18H_2O$. The diagram contains one non-variant point each – eutonics, which corresponds to saturation with pair of crystal-hydrates simultaneously. The diagram also contains very short branch of $PrCl_3 \cdot 7H_2O$ crystallization, and long branch of $C_{60}(OH)_{24} \cdot 18H_2O$, where the effect of fullerenol salt-out is distinctly observed.

Keywords: fullerene C_{60}, arginine, octo-adduct, lutetium chloride, solubility diagram, ternary system, simple eutonic.

Received: 6 April 2020

Revised: 29 May 2020

1. Introduction

This article continues the cycle of publications, concerning the synthesis, identification and physico-chemical, physical, bio-chemical, biological properties investigation of the amino-acid-light fullerene adducts [1–19]. This article is devoted to the investigation of the solubility diagram for systems containing water soluble fullerene nano-clusters, inorganic salt, including rare earth metals and actinoids, and water, as the solvent [20–24]. In prior research, it was shown, that water soluble fullerene nano-clusters (with amino-acid adducts, poly-hydroxylated forms – fullerenols, complex ethers with carboxylic acids) have a very strong salting-out effect at addition of inorganic salts or their crystal-hydrates, and the salting-out effect is most strongly pronounced for salts of 4-f and 5-f elements, somewhat weaker for the salts of d-elements, and even weaker for the salts of p- and s-elements. So, such 4-f element salts (as $PrCl_3$) may be effectively used for precipitation (by the salting-out effect) of fullerene nano-clusters (as $C_{60}(OH)_{24}$) and it is possible that separation from the matrix solution and purification occurs virtually without losses of nanoclusters. Currently, separation from the matrix solution and purification of fullerene nanoclusters is carried out, as a rule, by multistage (often triple) methanol (or methyl-acetate, or ethanol)-water recrystallization, which leads to the following:

- considerable losses of nanoclusters, because solubility of last ones in methanole with water impurities solutions is more or less considerable;
- nanoclusters for the same reasons contain a significant amount of impurities;
- recrystallization process itself is laborious.

2. Reagents

In the present investigation we used rare earth chloride $PrCl_3$, synthesized from the "chemical pure" oxide Pr_6O_{11} by treatment of "pure for the analysis" HCl with following vacuum drying. Fullerenol C_{60}–$C_{60}(OH)_{24}$ was synthesized by from the bromine derivative $C_{60}Br_{24}$ by the treatment of these product by boiling water-dioxane mixture with the dissolved NaOH. Then sodium fullerenes forms $C_{60}(OH)_{24-\delta}(ONa)_\delta$ were neutralized and washed in the

Soxlet-extractor bymethanol+HCl liquid phase. So, $PrCl_3$ and $C_{60}(OH)_{24}$ with purity $\approx$ 99.3 and 97.7 mass. %, correspondingly, were synthesized.

3. Experimental method

Solubility diagrams were investigated by the method of saturation in ampules at 25 ± 0.02 °C for 4 hours in the conditions of shaker-thermostate with shaking frequency of $\approx$ 2 Hz. For the prevention of Pr^{3+} precipitation in the form $Pr(OH)_3$, some drops of HCl was added to the heterogeneous systems, to approximate fixation of pH $\approx$ 3.0 – 3.5 a.un.

The concentration of $PrCl_3$ were determined by complexometric titration with trilon-B (disodium salt of ethylenediamine-tetraacetic acid – EDTA), titration conditions were the following: acetic buffer, indicator – 2 – 3 drops of 1-% Xylenol orange solution, color transition from violet to lemon-yellow [25].

Concentration of $C_{60}(OH)_{24}$ was determined with the help of absorption electronic spectroscopy according to optical density at wavelength $\lambda = 330$ nm – D_{330} (Ultraviolet-Visible Electronic Specto-photometer Shimadzu, wavelength $200 < \lambda < 900$ nm). Typical spectrum for $C_{60}(OH)_{24}$ water solution is represented in Fig. 1(a).

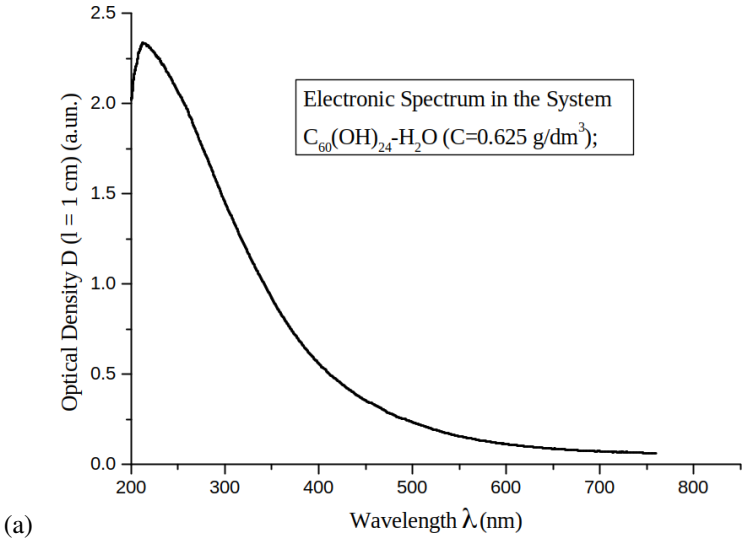

(a)

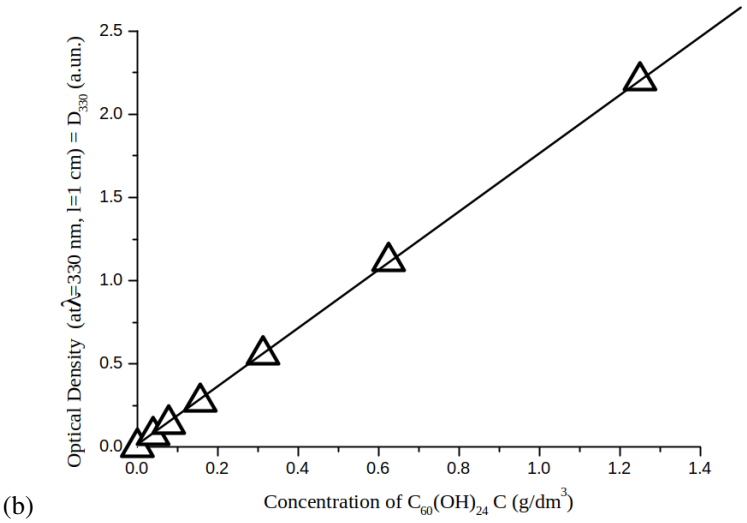

(b)

FIG. 1. Electronic spectrum of $C_{60}(OH)_{24}$ water solution (concentration of $C_{60}(OH)_{24}$ $C = 0.625$ g/dm^3) (a) and validity of Bouguer–Lambert–Beer Law in $C_{60}(OH)_{24}$ aqueous solutions at wavelength $\lambda = 330$ nm, optical path of $l = 1$ cm (b)

In Fig. 1(b), the validity of Bouguer–Lambert–Beer Law in $C_{60}(OH)_{24}$ water solutions in the nearest UV spectral diapazone is represented. One can see the almost complete linearity of the dependence of optical density at wavelength $\lambda = 330$ nm on the solution concentration. One can see, that, althought spectrum has no any expressed absorption

peaks, we can calculate $C_{60}(OH)_{24}$ concentration in g/dm^3, from optical density at wavelength $\lambda = 330$ nm, according to Bouguer–Lambert–Beer law by the formule:

$$C_{C60(OH)24}\ (\text{g/dm}^3)\ = 0.609 \cdot D_{330} \quad (l = 1\ \text{cm}). \tag{1}$$

Density of the solutions were determined with the help of quartz picnometers with operating volume $V \approx 5$ cm^3. Errors in the determination of $PrCl_3$ concentration was $\delta \approx 2.5$ relative %, $C_{60}(OH)_{24}$ $\delta \approx 5$ relative % , density $\delta \approx 0.1$ relative %.

4. Experimental data discussion

Solubility diagram in the ternary system $PrCl_3$–$C_{60}(OH)_{24}$–H_2O at 25 °C is represented in the Fig. 2 and Table 1. In Fig. 3, the dependence of the densities of saturated solutions in ternary system $PrCl_3$–$C_{60}(OH)_{24}$–H_2O at 25 °C is depicted.

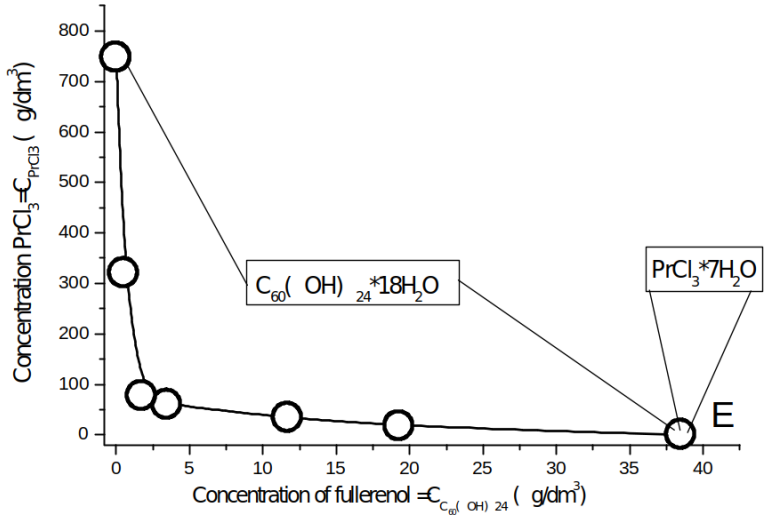

FIG. 2. Solubility in ternary system $PrCl_3$–$C_{60}(OH)_{24}$–H_2O at 25 °C

TABLE 1. Solubility in the $PrCl_3$–$C_{60}(OH)_{24}$–H_2O ternary system at 25 °C

Num	Density ρ (g/cm^3)	Optical density D (a.u.)	Concentration $C_{60}(OH)_{24}$ (g/dm^3)	Concentration $PrCl_3$ (g/dm^3)	Solid Phase
1	1.030	68.8	38.5	0.000	$C_{60}(OH)_{24} \cdot 18H_2O$
2	1.034	34.5	19.3	17.3	$C_{60}(OH)_{24} \cdot 18H_2O$
3	1.041	20.9	11.7	33.9	$C_{60}(OH)_{24} \cdot 18H_2O$
4	1.070	6.20	3.47	59.2	$C_{60}(OH)_{24} \cdot 18H_2O$
5	1.085	3.13	1.75	77.2	$C_{60}(OH)_{24} \cdot 18H_2O$
6	1.329	0.950	0.532	320	$C_{60}(OH)_{24} \cdot 18H_2O$
7	1.603	0.025	0.014	747	$C_{60}(OH)_{24} \cdot 18H_2O$+ $PrCl_3 \cdot 7H_2O$
8	1.603	—	0.000	747	$PrCl_3 \cdot 7H_2O$

The solubility diagram of in the $PrCl_3$–$C_{60}(OH)_{24}$–H_2O ternary system at 25 °C occurs due to simple eutonics [26–28], consisting of two branches, corresponds to crystallization of crystal-hydrates: $PrCl_3 \cdot 7H_2O$ and $C_{60}(OH)_{24} \cdot 18H_2O$. Diagrams contains one non-variant point – eutonics, which corresponds to saturation the pair of crystal-hydrates simultaneously. The diagram contains a very short branch for $PrCl_3 \cdot 7H_2O$ and a long branch for $C_{60}(OH)_{24} \cdot 18H_2O$ crystallization, where the effect of fullerenol salt-out is observed distinctly.

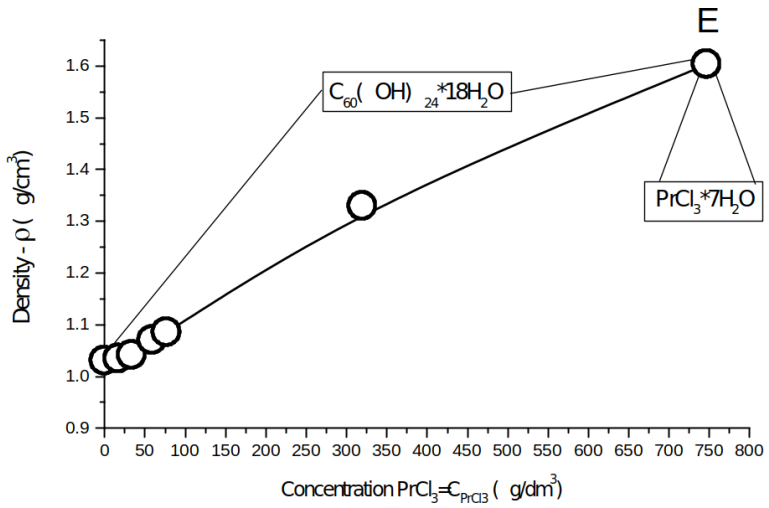

FIG. 3. Density of saturated solutions in the $PrCl_3$–$C_{60}(OH)_{24}$–H_2O ternary system at 25 °C

5. Interpretation of obtained solubility data according to empirical Sechenov equation and modified Debye equation

We also made an attempt to describe obtained solubility data according to the empirical Sechenov equation (eq. (2)) and modified Debye equation (eq. (3)):

$$\ln(C^0_{\mathrm{C60(OH)24}}/C_{\mathrm{C60(OH)24}}) = K_s C_{\mathrm{PrCl3}}, \tag{2}$$

where: $C^0_{\mathrm{C60(OH)24}}$ – solubility of non-electrolyte $C_{60}(OH)_{24}$ in H_2O, $C_{\mathrm{C60(OH)24}}$ – solubility of $C_{60}(OH)_{24}$ in ternary system, C_{PrCl3} – electrolyte $PrCl_3$ concentration, K_s – Sechenov empirical constant:

$$C^0_{\mathrm{C60(OH)24}}/C_{\mathrm{C60(OH)24}} = K_D C_{\mathrm{PrCl3}} + A C^{4/3}_{\mathrm{PrCl3}}, \tag{3}$$

where: K_D and A – fitting parameters of Debye model.

The results of approximation by Sechenov equation is represented in Fig. 4.

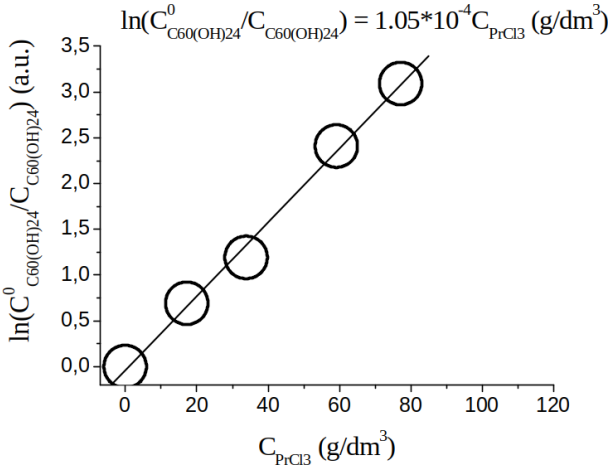

FIG. 4. Approximation of solubility diagram in ternary system $PrCl_3$–$C_{60}(OH)_{24}$–H_2O at 25 °C by Sechenov equation in the $0 < C_{\mathrm{PrCl3}} < 77.2$ g/dm^3 concentration range

From Fig. 4, one can see, that eq. (2) very precisely describes the crystallization curve of $C_{60}(OH)_{24} \cdot 18H_2O$. In more concentrated solutions ($77.2 < C_{\mathrm{PrCl3}} < 747$ g/dm^3) the descrepancy between calculated and experimental data increases many times, to our opinion, for the following reasons:

- $PrCl_3$ even remotely ceases to be a strong electrolyte (ion pairs and ion associates formation);
- $C_{60}(OH)_{24}$ in all saturated solutions it detects huge positive deviations from ideality by implementing a multi-stage sequential hierarchical association [29].

Exactly the same occurs when applying the Debye equation (3) – see Fig. 5, but the concentration range maybe considerably expanded: $0 < C_{\mathrm{PrCl3}} < 320$ g/dm^3 (calculation was provided with the help of software package Origin, subprogram Nonlinear curve fit).

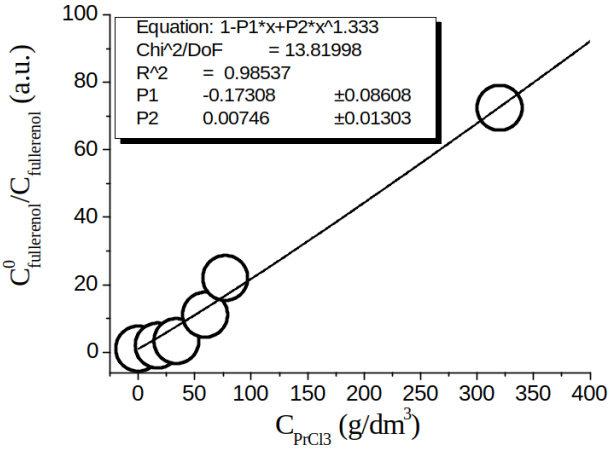

FIG. 5. Approximation of solubility diagram in ternary system $PrCl_3$–$C_{60}(OH)_{24}$–H_2O at 25 °C by Debye equation in concentration range $0 < C_{\mathrm{PrCl3}} < 320$ g/dm^3

6. Conclusions

The solubility diagram of the $PrCl_3$–$C_{60}(OH)_{24}$–H_2O ternary system at 25 °C occurs as simple eutonics, consisting of two branches, corresponding to crystallization of crystal-hydrates: $PrCl_3 \cdot 7H_2O$ and $C_{60}(OH)_{24} \cdot 18H_2O$. The diagram contains one non-variant point each – eutonics, which correspond to saturation with pair of crystal-hydrates simultaneously. The diagram also contains very short branch of $PrCl_3 \cdot 7H_2O$ crystallization, and long branch of $C_{60}(OH)_{24} \cdot 18H_2O$, where the effect of fullerenol salt-out is distinctly observed. The diagram in the range of low rare earth salt concentrations may be more or less precisely described by Sechenov or Debye equations.

Acknowledgements

This work was supported by Russian Foundation for Basic Research (RFBR) (Projects Nos. 18-08-00143 A, 19-015-00469 A, and 19-016-00003 A).

References

[1] Shestopalova A.A., Semenov K.N., et al. Physico-chemical properties of the C_{60}-arginine water solutions. *J. of Molecular Liquids*, 2015, **211**, P. 301–307.

[2] Semenov K.N., Charykov N.A., Keskinov V.A. Cryometry and excess functions of the adduct of light fullerene C_{60} and arginine – $C_{60}(C_6H_{13}N_4O_2)_8H_8$ aqueous solutions. *Nanosystems: Physics, Chemistry, Mathematics*, 2015, **6** (5), P. 715–725.

[3] Yur'ev G.O., Lelet M.I., et al. Thermodynamic and thermal properties of the C_{60}-L-Arg derivative. *J. Chem. Thermodynamics*, 2018, **127**, P. 39–44.

[4] Panova G.G., Serebryakov E.B., et al. Bioactivity Study of the C_{60}-L-Threonine Derivative for Potential Application in Agriculture. *Journal of Nanomaterials*, 2019, 2306518.

[5] Serebryakov E.B., Zakusilo D.N., et al. Physico-chemical properties of C_{70}-l-threonine bisadduct ($C_{70}(C_4H_9NO_2)_2$) aqueous solutions. *Journal of Molecular Liquids*, 2019, **279**, P. 687–699.

[6] Sidorov L.N., Yurovskaya M.A., et al. *Fullerenes: textbook. allowance*. M.: Exam, 2005, 668 p. (In Russian)

[7] Cataldo F., Ros T.Da. *Carbon Materials: Chemistry and Physics: Medicinal Chemistryand Pharmaco-logical Potential of Fullerenes and Carbon Nanotubes*. Springer, 2008, 372 p.

[8] Piotrovsky L.B., Kiselev O.I. *Fullerenes in biology*. Rostock, St. Petersburg, 2006, 336 p. (In Russian)

[9] Djordjevic A., Bogdanovic G., Dobric S. Fullerenes in biomedicine. *J. B.U.ON*, 2006, **11**, P. 391–404.

[10] Bianco C., Da Ros A., Prato T., Toniolo M. Fullerene-based amino acids and peptides. *J. Pept. Sci.*, 2001, **7**, P. 346–347.

[11] Jiang G., Yin F., Duan J., Li G. Synthesis and properties of novel water-soluble fullerene-glycine derivatives as new materials for cancer therapy. *J. Mater. Sci. Mater. Med.*, 2015, **26** (1), 5348.

[12] Grigoriev V.V., Petrova L.N., et al. Antioxidant properties of water soluble amino acid deriva-tives of fullerenes and their role in the inhibition of herpes virus infection. *Russ. Chem. Bull. Int.*, 2011, **60**, P. 1172–1176.

[13] Liang Bing Gan, Chu Ping Luo. Water-soluble fullerene derivatives, synthesis and characteriza-tion of ß-alanine C_{60} adducts. *Chinese Chemical letters*, 1994, **4** (5), P. 275–278.

[14] Safyannikov N.M., Charykov N.A., et al. Cryometry data in the binary systems bis-adduct of C_{60} and indispensable aminoacids – lysine, threonine, oxyproline. *Nanosustems: Physics, Chemistry, Mathematics*, 2018, **9** (1), P. 46–49.

[15] Serebryakov E.B., Semenov K.N., et al. Physico-chemical properties of the C_{70}-L-lysine aqueous solutions. *J. of Molecule Liquids*, 2018, **256**, P. 507–518.
[16] Semenov K.N., Iurev G.O., et al. Physico-Chemical properties of the C_{60}-L-lysine water solutions. *Journal of Molecular Liquids*, 2017, **225**, P. 767–777.
[17] Semenov K.N., Meshcheriakov A.A., et al. Physico-chemical and biological properties of C_{60}-L-hydroxyproline water solutions. *RSC Advances*, 2017, **7**, P. 15189–15200.
[18] Lelet M.I., Semenov K.N., et al. Thermodynamic and thermal properties of the C_{60}-L-lysine derivative. *J. Chem. Thermodynamics*, 2017, **115**, P. 7–11.
[19] Semenov K.N., Charykov N.A., et al. Physico-chemical properties of the C_{60}-L-threonine water solutions. *Journal of Molecular Liquids*, 2017, **242**, P. 940–950.
[20] Keskinov V.A., Semenov K.N., et al. Phase Diagrams of Fullerenol-d–$LaCl_3$–H_2O and Fullerenol-d–$GdCl_3$–H_2O Systems at 25 °C. *Russian Journal of Physical Chemistry A*, 2019, **93** (12), P. 2555–2558.
[21] Semenov K.N., Charykov N.A., et al. Phase equilibria in fullerene-containing systems as a basis for development of manufacture and application processes for nanocarbon materials. *Russ. Chem. Rev.*, 2016, **85** (1), P. 38–59.
[22] Pestov I.A., Keskinov V.A., et al. Solubility of $[C_{60}(=C(COOH)_2)_3]$ in the $[C_{60}(=C(COOH)_2)_3]$–$SmCl_3$–$H_{20}O$ Ternary System at 25 °C. *Russian Journal of Physical Chemistry A*, 2015, **89** (6), P. 998–1000.
[23] Semenov K.N., Charykov N.A. Solubility Diagram of a Fullerenol-d–NaCl–H_2O System at 25 °C. *Rus. J. Phys. Chem.*, 2012, **86** (10), P. 1636–1639.
[24] Semenov K.N., Keskinov V.A., et al. The fullerenol-d solubility in the fullerenol-d-inorganic salt-water ternary systems at 25 °C. *Industrial and engineering chemical research*, 2013, **52**, P. 16095–16100.
[25] Gschneidner K., Eyring L. *Handbook on physics and chemistry of rare earths*. Amsterdam, New York, Oxford: North-Holland Publishing Company, 1978.
[26] Korovin S.S., Zimina G.V., et al. *Rare and scattered elements. Chemistry and technology*. In 3 books. Book 1: Textbook for universities. Ed. Korovin S.S., M.: MISIS, 1996, 376 p. (In Russian)
[27] Charykov N.A., Charykova M.V., et al. Multiphase Open Phase Processes Differential Equations. *Processes*, 2019, **3** (7), P. 148–167.
[28] Charykova M.V., Charykov N.A. *Thermodynamic modeling of evaporite sedimentation processes*. St. Petersburg: Nauka, 2003, 262 p.
[29] Semenov K.N., Charykov N.A., et al. Fullerenols: Physicochemical properties and applications. *Progress in Solid State Chemistry*, 2016, **44** (2), P. 59–74.